Molecular Vision 2006; 12:125-41 <http://www.molvis.org/molvis/v12/a14/>
Received 4 November 2005 | Accepted 16 February 2006 | Published 27 February 2006

Gene expression profile of human trabecular meshwork cells in response to long-term dexamethasone exposure

Frank W. Rozsa,[1] David M. Reed,[1] Kathleen M. Scott,[1] Hemant Pawar,[1] Sayoko E. Moroi,[1] Theresa Guckian Kijek,[1] Charles M. Krafchak,[1,2] Mohammad I. Othman,[1] Douglas Vollrath,[3] Victor M. Elner,[1] Julia E. Richards[1,2]

Departments of [1]Ophthalmology and Visual Sciences and [2]Epidemiology, The University of Michigan, Ann Arbor, MI; [3]Department of Genetics, Stanford University, Stanford, CA

Purpose: Topical use of dexamethasone has long been associated with steroid induced-glaucoma, although the mechanism is unknown. We applied a strict filtering of comparative microarray data to more than 18,000 genes to evaluate global gene expression of cultured human trabecular meshwork cells in response to treatment with dexamethasone.
Methods: Three human trabecular meshwork cell primary cultures from nonglaucomatous donors were incubated with and without dexamethasone for 21 days. Relative gene expression was evaluated by analysis of U133A GeneChip and the results validated using quantitative polymerase chain reaction (PCR).
Results: Application of strict filtering to include only genes with statistically significant differences in gene expression across all three trabecular meshwork cell cultures produced a list of 1,260 genes. Significant changes in signal level were observed, including 23 upregulated and 18 downregulated genes that changed greater than three fold in each of three cell cultures. Using quantitative PCR we found changes greater than a thousand fold for two genes (SLP1 and SAA2) and changes greater than a hundred fold for another five genes (ANGPTL7, MYOC, SAA1, SERPINA3, and ZBTB16).
Conclusions: Expression changes in trabecular meshwork cells in response to dexamethasone treatment indicate that a group of actins and actin-associated proteins are involved in the development of cross-linked actin networks that form in response to dexamethasone. A trend was identified toward decreased expression of protease genes accompanied by an increased expression of protease inhibitors. Such a trend in nonproteasomal proteolysis conceivably affects gene product levels above the level of transcription. Only two genes, MYOC and IGFBP2, showed significantly elevated expression after dexamethasone treatment in our study and the other three previously published reports of primary culture trabecular meshwork cell gene expression.

Exposure to corticosteroids can cause elevated intraocular pressure (IOP) and can lead to open-angle glaucoma in susceptible individuals [1-6]. The presence of glucocorticoid receptors on the surface of trabecular meshwork (TM) cells suggests that the mechanism for steroid-associated glaucoma may operate through direct action on the (TM) cells in the outflow facility [7]. Treatment with dexamethasone leads to a variety of changes in TM cells including the formation of cross-linked actin networks (CLANs) within TM cells [8], altered levels of aqueous humor components including metal ions [9], increased levels of fibronectin and type IV collagen [10], and decreased expression of matrix metalloproteinases [11].

The myocilin (MYOC) gene is of special interest because it was initially identified by exposure of TM cells to dexamethasone over the course of weeks, a situation that models the rate at which elevated IOP develops in patients treated with dexamethasone [12,13]. Levels of myocilin protein are increased in TM in almost half of primary open-angle glaucoma (POAG) cases [14] even though mutations in MYOC coding sequences are present in less than 5% of POAG cases [15,16]. It is unclear whether elevated myocilin is causative or whether it is being produced in response to nonmyocilin components of the disease pathology.

Three previous microarray experiments, aimed at evaluating changes in gene expression in human TM cells in response to dexamethasone, identified different sets of genes [17-19]. Differences in the published gene expression findings may be the result of experimental variation and the small number of human genes screened.

We describe the global transcriptional response to long-term dexamethasone exposure for three different, fifth passage, primary human TM cell cultures. More than 13,000 human gene clusters were screened with the Affymetrix U133A GeneChip. A set of 111 genes was identified with three fold or greater change in expression in response to dexamethasone treatment. A subset of seven genes showed signal level increases in excess of a hundred fold, as verified by quantitative real-time polymerase chain reaction (qPCR). We discuss gene expression changes seen by ourselves and by others [17-19] that may be relevant to prior reports of dexamethasone-induced CLANs in TM cells [8], and highlight changes in growth factors, and proteins that affect proteolysis as important long-term responses of TM cells to dexamethasone.

METHODS

Eyes were obtained from the Midwest Eye-Banks (Ann Arbor, MI), which carried out informed consent and confirmed

Correspondence to: Julia E. Richards, Ophthalmology and Visual Sciences, Department of Epidemiology, The University of Michigan, Ann Arbor, MI; Phone: (734) 936-8966; FAX: (734) 615-0542; email: richj@umich.edu

that none of the donors had been diagnosed with glaucoma. Primary cultures of human TM cells, designated HTM A, HTM B, and HTM C, were grown from TM tissue samples dissected from the eyes of three Caucasian donors: a 12-year-old female, a 16-year-old male, and a 17-year-old female, respectively. Cells were grown according to conditions described previously [20,21]. Briefly, cells were grown in DMEM containing 15% fetal calf serum, supplemented with 1 ng/ml basic-fibroblast growth factor (bFGF) at 37 °C under 10% CO_2. After reaching confluency, cells were maintained for one week in 10% fetal calf serum without bFGF. For dexamethasone treatment, fifth passage TM cells were incubated in DMEM containing 10% fetal calf serum without bFGF with or without 100 nM dexamethasone for 21 days with media changes three times per week. TM cell type was confirmed by morphology and by dexamethasone-induction of expression of the MYOC gene, a hallmark of human TM cells [13]. Each of our three primary cultures of TM cells were assayed for myocilin coding sequence mutations by amplifying regions from genomic DNA using primers previously described [15,22] and with three additional sequencing primers; 5'-AGG CCA TGT CAG TCA TCC AT-3', 5'-CTG CTG AAC TCA GAG TCC CC-3', and 5'-GGC TCT CCC TTC AGC CTG CT-3'. No mutations or polymorphisms were detected in the MYOC coding region and adjacent splice sites for any of the three TM cell cultures.

Total RNA isolation: Following a 21-day-exposure to either dexamethasone-supplemented or untreated media, TM cells were harvested for RNA isolation. Flasks were washed three times in phosphate buffered saline (PBS), then Trizol (Invitrogen, Carlsbad, CA) reagent was added to lyse cells and solubilize RNA. Twenty percent (vol/vol) chloroform was added to each tube to separate aqueous and organic phases. One volume of 70% ethanol was added to the aqueous phase and purified over an RNAeasy column (Qiagen, Valencia, CA) following the manufacturer's protocol. The quality and quantity of the isolated RNA was evaluated by spectrophotometry and gel electrophoresis.

Preparation of cRNA: Double-stranded cDNA was generated from total RNA using the Superscript II Reverse Transcription kit (Invitrogen, Carlsbad, CA) according to the manufacturer's instructions, using oligo-dT primers (Qiagen Operon, Valenica, CA). Each product was purified using a GeneChip Sample Cleanup Module (Affymetrix, Santa Clara, CA). Purified cDNA was used as a template for in vitro transcription reactions using an RNA transcription labeling kit (Enzo Life Sciences, Farmingdale, NY) with biotin-16-UTP, biotin-11-CTP and unlabeled ATP, CTP, GTP, and UTP for 5 h at 37 °C. The cRNA was purified from unincorporated ribonucleotides with GeneChip Sample Cleanup Module (Affymetrix) columns. Biotinylated cRNA was fragmented in 1X fragmentation buffer (40 mM Tris acetate pH 8.1, 125 mM potassium acetate, 30 mM magnesium acetate) at 94 °C for 35 min. Spectrophotometric quantification and gel electrophoresis were used to determine quantity and quality of pre- and post-fragmented cRNA.

Oligonucleotide microarray hybridization: U133A (Affymetrix) GeneChips containing 22,215 probe sets representing 13,507 unique Unigene gene clusters (June, 2005 version) were incubated in prehybridization buffer (100 mM MES, 1 M NaCl, 20 mM EDTA, 0.01% Tween 20) at 45 °C for 10 min in a revolving rotisserie hybridization oven (Affymetrix). The prehybridization solution was replaced with 200 µl of hybridization solution containing fragmented cRNA (0.05 µg/µl) in 100 mM MES, 1 M NaCl, 20 mM EDTA, 0.01% Tween 20, acetylated BSA (0.5 mg/ml), herring sperm DNA (0.1 mg/ml), and biotinylated hybridization controls (Affymetrix) and incubated for 16 h at 45 °C. Prior to application, the hybridization mixture was denatured at 99 °C for 5 min, cooled for 5 min at 45 °C, and centrifuged at 16,000 times g for 5 min to remove particulates. Washing and staining of GeneChips were performed using the EukGE-WS2v4 protocol on a GeneChip Fluidics station 400 (Affymetrix) under nonstringent conditions at 25 °C in 6X SSPE (0.9 M NaCl, 60 mM NaH_2PO_4, 6 mM EDTA, and 0.01% Tween20) followed by a stringent wash at 50 °C in a solution of 100 mM MES, 0.1 M NaCl, and 0.01% Tween20. The washed arrays were stained in a solution of 100 mM MES, 1 M NaCl, 20 mM EDTA, 0.01% Tween 20, acetylated BSA (2 mg/ml), phycoerythrein-conjugated streptavidin (10 µg/ml, Molecular Probes, Eugene, OR) and incubated in an antibody solution containing 100 mM MES, 1 M NaCl, 20 mM EDTA, 0.01% Tween 20, BSA (2 mg/ml), normal goat IgG (Sigma-Aldrich, St. Louis, MO; 100 µg/ml), and biotinylated antibody (3 µg/ml; Vector Laboratories, Burlingame, CA). Fluorescence was quantified by an Affymetrix GeneChip 3000 scanner.

Microarray analysis: Gene expression was quantified for each primary culture using two biological replicates (from separate flasks of cells) plus one technical replicate (from two different labelings of the same RNA preparation) for both untreated and dexamethasone-treated cells. Three biological replicates were used for the untreated HTM B cells. The expression analysis algorithm in Affymetrix Microarray Analysis Suite 5.1 (MAS5.1) was used for absolute analysis of the computed cell averages and to determine whether each probe was present, absent, or marginally present for each GeneChip. Marginal calls were treated as present calls in further analysis. Data from all U133A GeneChips were scaled to an average intensity of 1500 using all probe sets prior to importing the results into Affymetrix Data Mining Tool 3.0 software (DMT3.0). Additional comparative analyses such as relative fold change calculations and Mann-Whitney statistics were performed in DMT3.0. Scatterplots were drawn in Spotfire DecisionSite 8.0 software (Spotfire Inc., Cambridge, MA) using a base 10 log-log plot of the GeneChip signal intensities. Averaged signal intensities from single or multiple cell cultures were used for generating scatterplots. Genes corresponding to probes of interest were identified by processing the probe identifiers through the Affymetrix NetAffx [23], MatchMiner [24], and DAVID [25] databases to extract public database information for each probe. In cases where a gene was represented by multiple probes, the probe that produced

the highest fold change (untreated compared to dexamethasone-treated) was retained. Affymetrix probes that cross-hybridize to other sequences (probes with an "_x" suffix) were excluded if a more reliable probe was available. Data noise was evaluated by scatterplot comparisons of the biological replicates for each cell culture within the same treatment group (untreated compared to untreated, and dexamethasone-treated compared to dexamethasone-treated). Additional analyses of expression levels on Affymetrix U133A GeneChips were performed using the Robust Multi-array Average (RMA) method in GeneSifter (VizXlabs, Seattle, WA) with a t-test p value of 0.005 as the breakpoint between significant and nonsignificant changes in expression. RMA calculates expression levels based only on the perfect-match probe signals [26] and uses a quantile normalization method to produce signals with identical distributions [27]. Genes are denoted by the gene symbols found in the Affymetrix database and cross-referenced to probesets and GenBank accession numbers.

Data filtering: The fold change for each probe was calculated from the averaged data for each TM cell culture and the entire data set using DMT3.0. Significant change in gene expression was calculated from the entire unstratified data using the nonparametric Mann-Whitney test in DMT3.0. Probes were considered to have a statistically significant change in gene expression if the computed p value was less than 0.005. Probes with p values greater than or equal to 0.005 were excluded from further analyses.

To analyze only genes consistently expressed in at least one treatment condition across all donors, we eliminated probes with insufficient signal in both untreated and dexamethasone-treated cells. Analysis to exclude probes absent in both conditions was usually performed using MAS5.1 with pairs of GeneChips, but this approach cannot be used when assessing composite data from multiple cell cultures. Instead, we used strict criteria to define a probe as "absent" for each condition for the average of every individual TM cell culture. A probe was considered absent for the individual cell culture and treatment condition only if MAS5.1 identified the probe as absent for every GeneChip in a treatment condition; otherwise the probe was considered present. If any probe was absent for both untreated and dexamethasone-treated GeneChip data for any single TM cell culture then it was excluded from further analyses. The remaining present or absent calls were calculated for the composite data using the majority call from the three individual cell culture averages.

Probes with at least a three fold change in the composite data set were identified from a pool of probes found to be statistically significant and considered present in at least one treatment group. At this point, duplicates were removed, so that multiple probes corresponding to the same gene were counted only once. To produce the most stringent list of genes, we identified unique probes that produced not only a three fold or greater change in expression in the composite data set but also a three fold or greater change in every individual TM cell culture. The changes in gene expression were validated using quantitative PCR.

Quantitative polymerase chain reaction: Gene expression levels (Table 1) were measured using the comparative threshold method. Intron-spanning primers were used to amplify samples for fluorescence in an iQ SYBR Green Supermix reaction (Bio-Rad Laboratories, Hercules, CA) in an iCycler (Bio-Rad) equipped with an optical module (Bio-Rad) according to the manufacturer's instructions. cDNA was prepared from the same preparation of RNA used in the microfluidics analysis described as follows, and each assay contained cDNA derived from 25 ng of total RNA from the same preparation of RNA used in the GeneChip experiment. Thermal cycling conditions were 10 min at 95 °C, followed by 45 cycles of: 30 s at 95 °C, 30 s at 58 °C, 30 s at 75 °C, and final extension step for 6 min at 72 °C. Cycle threshold values (C_T) values were cal-

Table 1. Primers used for quantitative polymerase chain reaction

Gene title (Symbol)	Forward primer	Reverse primer
aldehyde oxidase 1 (AOX1)	ATCCCTGCCATCTGTGACATG	ATCTGGGAAGAGGCACTCTGT
bone morphogenetic protein 2 (BMP2)	GCTGTCTTCTAGCGTTGCTG	GTGATAAACTCCTCCGTGGG
chromosome 9 open reading frame 26 (C9orf26)	GACTTCTGGTTGCATGCCAAC	CCCTTAGATGTCACCTGTCTC
chitinase 3-like 1 (CHI3L1)	TGCCAGTAAGCTGGTGATGG	TGCTGTGTGCAGAACAGAGG
ceruloplasmin (CP)	TCCCAGAAAGATCTGGAGCTG	AGGGTTTGGTATGTTCCAGGG
Coxsackie virus and adenovirus receptor (CXADR)	TGCCCACTTCATGGTTAGCAG	TGTTGGAAGGAGACATGGACC
EphA4 (EPHA4)	GCTATGTGCATCGTGATCTGG	CCAACATGTTGACAATCTGCC
glyceraldehyde-3-phosphate dehydrogenase (GAPDH)	TCCACCACCCTGTTGCTGTAG	GACCACAGTCCATGACATCACT
gastrin-releasing peptide (GRP)	AAGAGCACAGGGGAGTCTTCT	GATGATCCGTAGAACTGATGC
insulin-like growth factor II (IGF2)	GCTTCTCACCTTCTTGGCCT	GGACTGCTTCCAGGTGTCAT
integrin, beta-like 1 (ITGBL1)	ATGTTCCTGTGGTCGCTGTG	TCCATTCCATCCATCCCAGC
lumican (LUM)	TCAGATAGCCAGACTGCCTTCT	GAGTGACTTCGTTAGCAACACG
metallothionein 1M (MT1M)	CTAGCAGTCGCTCCATTTATCG	CAGCTGCAGTTCTCCAACGT
nebulette (NEBL)	GCAAAGCCATTCCCAAGGCT	CCTGGTACCTGTGTGTCTAA
purinergic receptor P2Y, G-protein coupled, 14 (P2RY14)	ACACTTGGGCCACTTCAAGAC	CCTGAGTCACCAAGGATCTTG
proprotein convertase subtilisin/kexin type 1 (PCSK1)	CGGGATACATCTCCTAATGGC	GAAAGCACTTTGCAGGAGTCG
period homolog 1 (PER1)	TCTGTGCTGAAGCAGGATCG	CTGGTGCAGTTTCCTGCTGT
phosphorylase, glycogen; brain (PYGB)	AGATCCAGCATGCAAGGTGCT	TGCTGTGTCCTGAGGTGCATT
serum amyloid A1 (SAA1)	CTATGATGCTGCCAAAAGGGG	TACCCTCTCCCCGCTTTGTA
serum amyloid A2 (SAA2)	CTATGATGCTGCCAAAAGGGG	CAGCTTCTCTGGACATAGACC

Genes not present on the microfluidics card were assayed by quantitative realtime PCR using the primers (5' to 3') described.

culated by the iCycler iQ Optical System Software 3.0 (Bio-Rad) and compared to GAPDH controls. Selection of any one standardly-used control gene for such experiments must take into account the issue of whether the control gene is itself showing differences in signal level under the conditions being compared. GAPDH was deemed a reasonable control given that treated-to-untreated ratios for the three different GAPDH probes on the GeneChip ranged from 1.074 to 1.111, with those ratios found by Mann-Whitney test not to be significantly different from a ratio of 1 (p values range from 0.165 to 0.327). PCR product was confirmed to be a single band for each gene tested by melt curve analysis, visualization of single-band PCR products using agarose gel electrophoresis that correspond to the predicted size for each gene assayed (data not shown). Three, or more, replicates were performed for each gene assayed.

Other qPCR confirmations were carried out using a custom-designed TaqMan Low Density Array (Applied Biosystems, Foster City, CA). GAPDH controls and the 52 genes listed in Table 2 were represented twice on the microfluidic array. Templates for microfluidic qPCR samples were prepared from the same total RNA as the Affymetrix GeneChip experiments. For each treatment condition, cDNA created from 200 ng of total RNA via High Capacity cDNA Archive kit (Applied Biosystems) was mixed with 2X TaqMan Universal Mix (Applied Biosystems) and applied to the microfluidic card. Thermal cycling was carried out for 40 cycles of 15 s at 95 °C, 60 s at 60 °C. Capture of fluorescence was recorded on the ABI Prism 7900HT scanner, and the C_T was calculated for each assay using Sequence Detection System Software 2.1 (Applied Biosystems). The C_T values for each microfluidic assay were compared to the C_T values for GAPDH controls, allowing a fold change calculation to be made relative to the untreated sample. Two microfluidic cards were assayed for each TM cell culture to compile an average fold change in transcript level detected for each individual cell culture and a composite average. Affymetrix GeneChip findings were considered validated if the microfluidic (qPCR) results from each individual cell culture were greater than three fold.

Classification of genes into gene families: Genes with statistically significant findings ($p<0.005$ by Mann-Whitney test) were classified into gene families using the Ingenuity Pathways Knowledge Base database (Ingenuity Systems Inc., Mountain View, CA), a web-delivered application that enables biologists to discover, visualize, and explore therapeutically relevant networks significant to their experimental results, such as gene expression array data sets (Ingenuity). Genes absent from the Ingenuity database were classified using the NetAffyx Gene Ontology [23] or DAVID [25] classification databases or from the literature. Some Ingenuity gene family categories were pooled into a single category, such as G-protein-coupled receptors and transmembrane receptors.

RESULTS

Comparison of data from 19 U133A GeneChips: Three different primary human TM cell cultures were exposed to a 21-day course with and without dexamethasone treatment. Total RNA was isolated and examined for changes in gene expression using high-density oligonucleotide microarrays (Affymetrix). A total of 19 Affymetrix U133A GeneChips were assayed, three per condition for each cell culture with the exception of untreated HTM B, which was assayed using four GeneChips. The average signal intensity of 3686 and 225 for present and absent categories, respectively, was similar for all combinations of cell culture and treatment. About 54% of the probes were assigned a status of present in both the untreated and dexamethasone-treated composite average while 44% were assigned a status of absent under both conditions. The remaining probes were considered absent in one condition and present in the other. There was little change in the percentages of genes assigned to the different presence/absence categories across the different cell cultures (Figure 1).

Comparison of microarray data from similar treatments: To determine if there were excess variation between microarray signals derived from different preparations of RNA from the same cell culture and treatment, signal intensity scatterplots from two individual untreated samples (Figure 2A) were compared to two dexamethasone-treated samples (Figure 2B). Similar distributions of signal intensities were observed between the same treatment groups in cell cultures HTM A and HTM B (data not shown). As seen in Figure 2A and Figure 2B, most of the spread in the data occurs at low signal intensities (approximately less than 200) in the lower left quadrant of the scatterplot. These low signal intensities typically correspond to probes that are identified as absent by the MAS5.1 software and are excluded from further analyses. A few of the low signal probes, identified as present, have a three fold or greater change when two samples from one cell culture were compared (untreated compared to untreated, or dexamethasone-treated compared to dexamethasone-treated). However, none of these outliers were consistently present in other similarly treated TM cell cultures.

Comparison of microarray data from dexamethasone and untreated samples: Nine Affymetrix U133A GeneChips were prepared from three TM cell cultures that were incubated for 21 days in the presence of dexamethasone and compared to ten U133A GeneChips prepared from untreated TM cells. Signal intensities from a single dexamethasone-treated sample compared to a single untreated sample from the same cell culture (Figure 3A) shows more variation around the central line (y=x) of no change relative to cells with the same treatment (Figure 2A,B). In all cases, the data are distributed symmetrically around the line representing (y=x), or no change. Variation reduces when average signal intensities of three GeneChips for each treatment group in one cell culture are combined (Figure 3B). Plots of the average signal intensities from all untreated samples against all dexamethasone-treated samples produced less variation than any individual TM cell culture (Figure 3C).

Probes without a statistically significant change in signal level ($p<0.005$, Mann-Whitney test for the composite data) were removed, leaving 1,776 probes remaining. Further exclusion of duplicate and absent probes reduced the list of genes

Table 2. Validation of microarray results by quantitative PCR

A:

Affymetrix probe	GenBank	Gene title (symbol)	Microarray fold change	qPCR fold change	Microarray signal mean untreated	Microarray signal mean dex-treated
214456_x_at	M23699	serum amyloid A1 (SAA1)	218.7	338.4*	91 (A)	19873 (P)
206423_at	NM_021146	angiopoietin-like 7 (ANGPTL7)	187.0	365.3	112 (A)	20939 (P)
208607_s_at	NM_030754	serum amyloid A2 (SAA2)	114.0	2852.0*	56 (A)	6405 (P)
202376_at	NM_001085	serine (or cysteine) proteinase inhibitor, clade A, member 3 (SERPINA3)	48.2	150.9	1436 (P)	69260 (P)
203021_at	NM_003064	secretory leukocyte protease inhibitor (SLPI)	34.2	1706.8	527 (A)	18023 (P)
204363_at	NM_001993	coagulation factor III (F3)	26.2	15.9	137 (A)	3592 (P)
205403_at	NM_004633	interleukin 1 receptor, type II (IL1R2)	22.9	26.4	44 (A)	1000 (P)
204560_at	NM_004117	FK506 binding protein 5 (FKBP5)	19.9	6.5	144 (A)	2873 (P)
210155_at	D88214	myocilin, trabecular meshwork inducible glucocorticoid response (MYOC)	16.7	191.3	4688 (P)	78368 (P)
205883_at	NM_006006	zinc finger and BTB domain containing 16 (ZBTB16)	13.6	734.3	365 (A)	4950 (P)
212741_at	AA923354	monoamine oxidase A (MAOA)	13.1	16.2	353 (A)	4612 (P)
218723_s_at	NM_014059	response gene to complement 32 (RGC32)	12.3	17.5	1441 (P)	17743 (P)
206024_at	NM_002150	4-hydroxyphenylpyruvate dioxygenase (HPD)	11.9	7.7	1018 (P)	12132 (P)
221541_at	AL136861	cysteine-rich secretory protein LCCL domain containing 2 (CRISPLD2)	10.6	12.9	706 (P)	7459 (P)
217546_at	R06655	metallothionein 1M (MT1M)	8.9	36.8*	486 (A)	4297 (P)
202409_at	X07868	insulin-like growth factor II (IGF2)	7.8	32.2*	384 (P)	2987 (P)
208763_s_at	AL110191	TSC22 domain family, member 3 (TSC22D3)	6.8	8.8	1496 (P)	10171 (P)
205422_s_at	NM_004791	integrin, beta-like 1 (ITGBL1)	6.4	9.4	760 (P)	4883 (P)
201525_at	NM_001647	apolipoprotein D (APOD)	5.3	16.0	2920 (P)	15340 (P)
200974_at	NM_001613	actin, alpha 2, smooth muscle, aorta (ACTA2)	4.6	8.4	8108 (P)	37623 (P)
203961_at	AL157398	nebulette (NEBL)	4.4	12.0	145 (A)	642 (P)
204627_s_at	M35999	integrin, beta 3 (ITGB3)	3.9	4.6	188 (A)	737 (P)
204326_x_at	NM_002450	metallothionein 1X (MT1X)	3.7	5.9	10597 (P)	39047 (P)

B:

Affymetrix probe	GenBank	Gene title (symbol)	Microarray fold change	qPCR fold change	Microarray signal mean untreated	Microarray signal mean dex-treated
209821_at	AB024518	chromosome 9 open reading frame 26 (C9orf26)	-17.1	-92.6*	1850 (P)	108 (P)
209541_at	AI972496	insulin-like growth factor 1 (IGF1)	-13.1	-34.8	3515 (P)	268 (P)
205825_at	NM_000439	proprotein convertase subtilisin/kexin type 1 (PCSK1)	-11.7	-12.5*	6342 (P)	544 (P)

Table 2. Continued.

Affymetrix probe	GenBank	Gene title (symbol)	Microarray fold change	qPCR fold change	Microarray signal mean untreated	Microarray signal mean dex-treated
210119_at	U73191	potassium inwardly-rectifying channel, subfamily J, member 15 (KCNJ15)	-8.8	-12.8	2715 (P)	308 (P)
204948_s_at	NM_013409	follistatin (FST)	-8.7	-20.7	21126 (P)	2443 (P)
206022_at	NM_000266	Norrie disease (NDP)	-7.7	-34.7	2036 (P)	265 (P)
221577_x_at	AF003934	growth differentiation factor 15 (GDF15)	-7.3	-7.3	6564 (P)	897 (P)
206326_at	NM_002091	gastrin-releasing peptide (GRP)	-6.8	-34.8*	3806 (P)	562 (A)
205266_at	NM_002309	leukemia inhibitory factor (LIF)	-6.8	-13.3	4422 (P)	655 (P)
204933_s_at	NM_002546	tumor necrosis factor receptor superfamily, member 11b (TNFRSF11B)	-6.6	-11.3	3312 (P)	500 (A)
204135_at	NM_014890	downregulated in ovarian cancer 1 (DOC1)	-5.9	-9.1	6348 (P)	1084 (P)
210511_s_at	M13436	inhibin, beta A (INHBA)	-4.8	-6.3	7409 (P)	1554 (P)
201830_s_at	NM_005863	neuroepithelial cell transforming gene 1 (NET1)	-4.4	-5.8	3943 (P)	897 (P)
204846_at	NM_000096	ceruloplasmin (CP)	-4.3	-5.2*	662 (P)	153 (A)
205127_at	NM_000962	prostaglandin-endoperoxide synthase 1 (PTGS1)	-4.3	-8.2	1064 (P)	246 (A)
209960_at	X16323	hepatocyte growth factor (HGF)	-4.2	-7.5	5066 (P)	1218 (P)
205207_at	NM_000600	interleukin 6 (interferon, beta 2) (IL6)	-3.7	-4.6	4562 (P)	1231 (P)
205289_at	AA583044	bone morphogenetic protein 2 (BMP2)	-3.6	-4.4*	779 (P)	215 (P)

C:

Affymetrix probe	GenBank	Gene title (symbol)	Microarray fold change	qPCR fold change	signal mean untreated	Microarray signal mean dex-treated
206637_at	NM_014879	purinergic receptor P2Y, G-protein coupled, 14 (P2RY14)	7.5	2.4*	103 (A)	772 (P)
201481_s_at	NM_002862	phosphorylase, glycogen; brain (PYGB)	6.9	1.7*	743 (A)	5111 (P)
206114_at	NM_004438	EPH receptor A4 (EPHA4)	6.4	2.3*	341 (A)	2201 (P)
205082_s_at	AB046692	aldehyde oxidase 1 (AOX1)	5.5	2.4*	649 (P)	3551 (P)
208613_s_at	AV712733	filamin B, beta (FLNB)	4.8	2.9	534 (A)	2557 (P)
219028_at	NM_022740	homeodomain interacting protein kinase 2 (HIPK2)	4.3	3.0	768 (P)	3298 (P)
205547_s_at	NM_003186	transgelin (TAGLN)	3.5	3.4	12015 (P)	42093 (P)
202861_at	NM_002616	period homolog 1 (PER1)	3.4	8.8*	278 (A)	954 (P)
201744_s_at	NM_002345	lumican (LUM)	-4.8	-9.9*	8833 (P)	1861 (P)
216546_s_at	AJ251847	chitinase 3-like 1 (CHI3L1)	-6.1	-2.7*	3101 (P)	505 (A)
203917_at	NM_001338	coxsackie virus and adenovirus receptor (CXADR)	-7.2	-7.1*	8188 (P)	1139 (P)

A: Genes with three fold increase in signal intensity after dexamethasone treatment by both microarray and qPCR analysis for all three TM Cell lines. **B**: Genes with three fold decrease in signal intensity after dexamethasone treatment by both microarray and qPCR analysis for all three TM cell lines. **C**: Genes with a qPCR fold change less than three fold in one or more TM cell lines. Quantitative PCR performed using intron-spanning primers are shown by asterisks. In the microarray analysis (P) and (A) indicate whether the signal was scored as present or absent, respectively.

considered present in one or both treatment to 1,260 genes (Figure 3D, Appendix 1). Of these, 111 genes had a three fold or greater change for the composite averaged data (Table 3), while 52 genes showed three fold or greater change in each of the three TM cell cultures (Table 2 and Figure 4). All 52 of these genes also showed significant changes in expression when analyzed using the RMA methodology.

Quantitative polymerase chain reaction results: Changes of more than three fold in the GeneChip data for the 52 genes in Table 2 were confirmed using qPCR with intron-spanning primers or commercially prepared microfluidic cards (Applied Biosystems). Microarray findings for 41 genes were considered validated by qPCR results that demonstrated at least a three fold change for all three individual cell cultures and the composite average (Table 2A,B).

Seven genes produced fold-change increases in excess of one hundred fold by qPCR (ANGPTL7, MYOC, SAA1, SAA2, SERPINA3, SLP1, and ZBTB16), with two of these showing increases in excess of a thousand fold (SLP1 and SAA2, Table 2A). The greatest decrease in signal was C9orf26 with a decrease of -92.6 fold (Table 2B). Eleven of the 52 genes had less than three fold change in signal by qPCR in at least one of the three cell cultures (Table 2C). None of these 11 genes demonstrated qPCR data that conflicted with the signal directional change (increase or decrease) from Affymetrix U133A GeneChips in the composite data (Table 2C). Five genes (CXADR, HIPK2, LUM, PER1, and TAGLN) had fold changes by qPCR less than three fold in one TM cell culture, even though the composite average change met or exceeded three fold (data not shown). GeneChip and qPCR fold-change findings were highly correlated (r^2=0.887). Hence, GeneChip findings for other genes in this study should be qualitatively

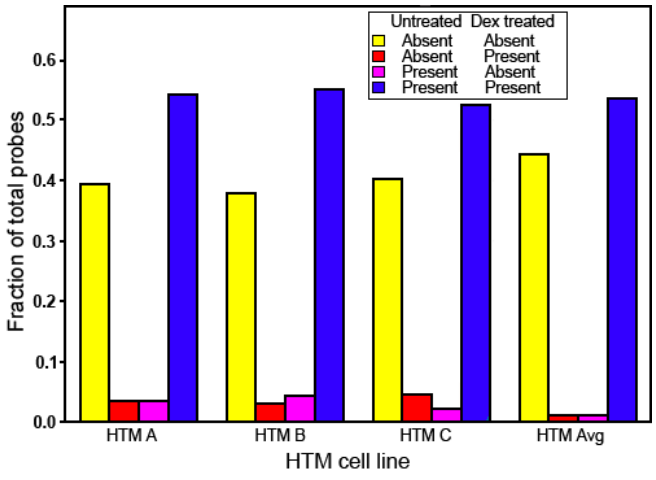

Figure 1. Microarray presence or absence calls in three human trabecular meshwork cell cultures. Untreated and dexamethasone-treated human TM cell cultures were analyzed by Affymetrix U133A microarrays and the average number of probes in each category recorded for each individual cell culture. Probes were scored; absent:absent, absent:present, present:absent, or present:present (untreated:dexamethasone-treated), using MAS5.1 software as described in the Methods. The fraction of the number of probes in each category compared to the total number of probes is shown as bars for each cell culture. A composite average comparing all untreated to all dexamethasone-treated cell cultures is shown on the right.

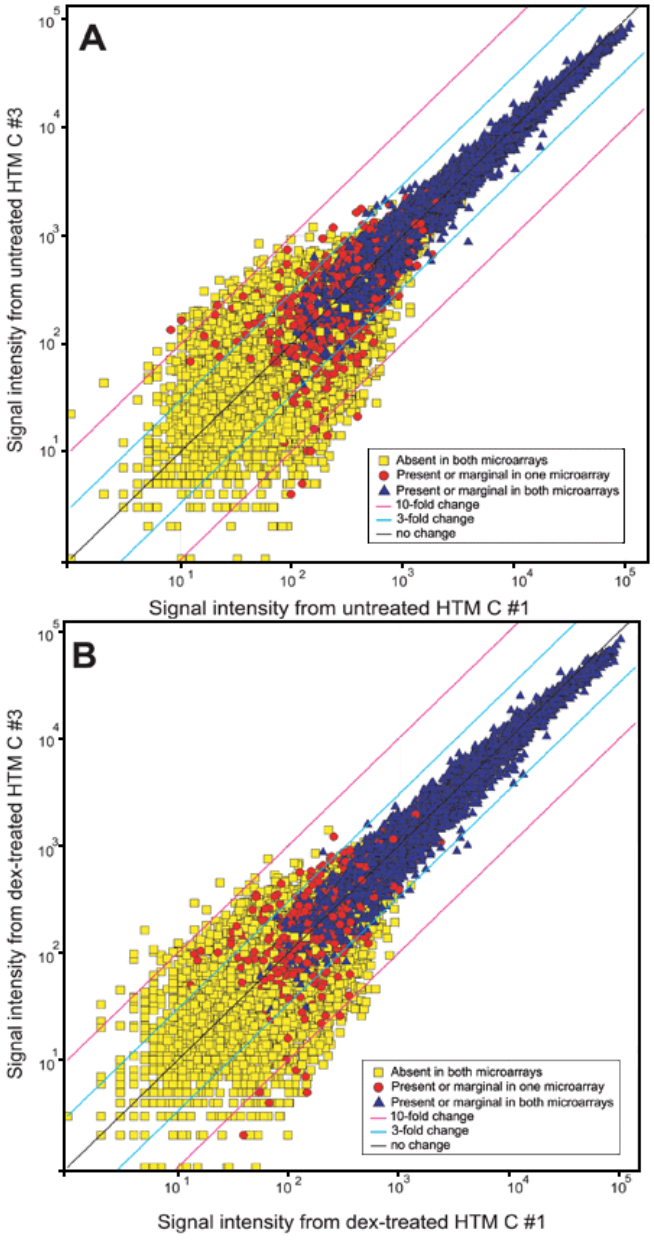

Figure 2. Scatterplots of signal intensities comparing human trabecular meshwork cell cultures with the same treatment status. **A**: GeneChip data from two different untreated HTM C cultures. **B**: GeneChip data from two different dexamethasone-treated HTM C cultures. Axes indicate the logarithmic signal intensity corresponding to each probe. Color coding and symbols shown in the key indicate present-absent status based on MAS5.1 software analysis (see Methods). Yellow squares represent probes called absent in both data sets, blue triangles were called present or marginal in both data sets, and red circles were called present or marginal in one data set and absent in the other. Black, light blue, and pink diagonal lines represent change boundaries of no change, three fold, and ten fold change, respectively.

correct, even though absolute change levels are different. Many of the largest differences between GeneChip and qPCR findings occur when one, or both of the signal levels are very high (i.e., near the saturation point for the microchip readings), or when one of the signals is low and denoted as absent by MAS5.1. For low readings deemed absent, the actual level of transcript present may fall below the level of sensitivity of the GeneChip detection system (Table 2) and a change from absent to present or from present to absent may represent initiation or elimination of gene expression rather than a qualitative increase or decrease of expression.

Classification of genes with altered signal levels: The 1,260 genes (Figure 3D, Appendix 1) showing significant changes in expression after a 21-day exposure to dexamethasone were classified into functional categories as afore described. The number of genes that were increased or decreased in expression (relative to untreated) was sorted for each category to determine if the directional change in expression of a functional category is statistically different (Figure 5A). Out of the 19 functional categories for 1,260 significantly changed genes, 8, 9, and 13 categories had a significant difference between increased and decreased expression using significance levels of $p<0.005$, 0.01, and 0.05, respectively (Figure 5A). A subset of these data, 111 genes with significant and greater than three fold change in signal level (Table 3) encompassed fewer, but nearly all, of the functional categories of the greater set (Figure 5B). Statistical differences between increased and decreased signal changes within each category only are only present for one category at $p<0.05$. In Figure 5C, we observe that 13 of the original 19 categories are represented for the 41 genes that were validated by qPCR and showed a greater than three fold change in expression in all three TM cell cultures (Table 2A,B). Only the growth factor category shows a significant difference ($p=0.006$) between the number of genes with increased expression and the number of genes showing decreased expression.

Expression of myocilin: MYOC gene expression was induced in all TM samples tested, an expected result because MYOC was originally cloned based on its induction by dexamethasone [12]. MYOC signal intensities showed a composite average increase of 17 fold by GeneChip, but larger fold changes, averaging 191 fold, were observed by qPCR (Table 2) suggesting that MYOC levels may exceed the upper thresh-

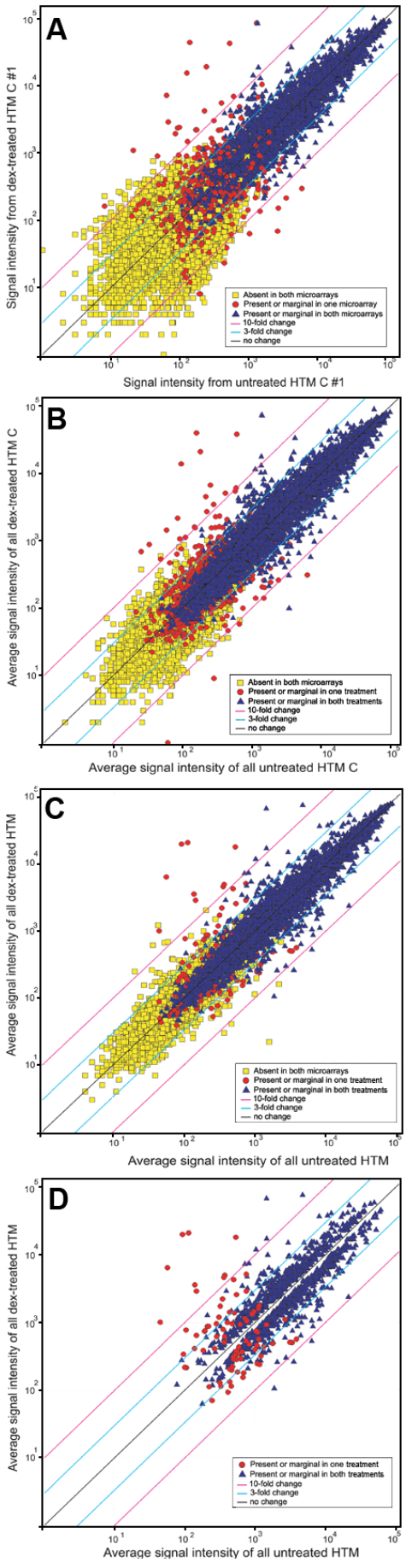

Figure 3. Scatterplots of signal intensities in human trabecular meshwork cells with different treatment. **A**: Data from one GeneChip from dexamethasone-treated HTM C and data from one GeneChip from untreated HTM C. **B**: Average signal intensities of data from three GeneChips from three dexamethasone-treated HTM C samples and the average signal intensities of data from three GeneChips from three untreated HTM C samples. **C**: Average signal intensities of data from nine GeneChips from all dexamethasone-treated TM samples and the average signal intensities of data from 10 GeneChips from all untreated TM samples. **D**: Data from Panel **C** after removal of duplicate, nonsignificant, or absent probes as described in Methods. Black, light blue, and pink diagonal lines represent change boundaries of no change, three fold, and ten fold change, respectively.

Table 3. 111 Differential dexamethasone-induced gene expression in trabecular meshwork, sorted by functional categories

GenBank	Gene title (Symbol)	HTM A fold	HTM B fold	HTM C fold	Mean fold
Adhesion					
NM_004791	integrin, β-like 1 (IGBL1)	8.4	4.4	7.5	6.4
M35999	integrin, β3 (ITGB3)	4.7	3.2	4.4	3.9
BC003610	milk fat globule-EGF factor 8 protein (MFGE8)	2.8	2.2	5.7	3.3
AW188198	tumor necrosis factor, α-induced protein 6 (TNFAIP6)	-5.1	-6.8	-1.9	-3.8
Cytokine					
NM_000600	interleukin 6 (IL6)	-4.1	-3.1	-4.1	-3.7
NM_002309	leukemia inhibitory factor (LIF)	-7.6	-5.8	-7.1	-6.8
Cytoskeleton					
NM_001615	actin, γ2, smooth muscle, enteric (ACTG2)	2.9	19.2	4.2	9.4
AV712733	filamin B, β (FLNB)	4.2	3.5	6.8	4.8
NM_001613	actin, α2, smooth muscle, aorta (ACTA2)	4.8	4.1	5.2	4.6
AL157398	nebulette (NEBL)	3.3	4.9	7.2	4.4
AL136139	neural precursor cell expressed, developmentally downregulated 9 (NEDD9)	4.7	3.0	6.2	4.3
NM_003186	transgelin (TAGLN)	3.4	3.4	4.8	3.5
Enzyme					
NM_004117	FK506 binding protein 5 (FKBP5)	104.4	19.3	12.4	19.9
AA923354	monoamine oxidase A (MAOA)	17.1	13.3	9.6	13.1
NM_002150	4-hydroxyphenylpyruvate dioxygenase (HPD)	14.4	5.4	13.3	11.9
NM_002862	phosphorylase, glycogen; brain (PYGB)	8.9	5.4	21.0	6.9
AB046692	aldehyde oxidase 1 (AOX1)	5.4	3.4	6.8	5.5
NM_018063	helicase, lymphoid-specific (HELLS)	6.3	3.8	1.3	4.0
NM_021154	phosphoserine aminotransferase 1 (PSAT1)	5.0	4.7	2.2	3.8
NM_016341	phospholipase C, epsilon 1 (PLCE1)	5.0	2.4	3.3	3.6
NM_014863	B cell RAG associated protein (GALNAC4S-6ST)	5.5	2.3	2.9	3.3
AI479175	sulfatase 1 (SULF1)	-1.5	-6.1	-5.5	-3.0
NM_018371	chondroitin β1,4 N-acetylgalactosaminyltransferase (ChGn)	-2.4	-4.0	-2.4	-3.2
NM_000691	aldehyde dehydrogenase 3 family, member A1 (ALDH3A1)	-5.0	-5.9	-2.3	-3.3
NM_005019	phosphodiesterase 1A, calmodulin-dependent (PDE1A)	-2.9	-5.8	-2.7	-3.8
NM_000962	prostaglandin-endoperoxide synthase 1 (PTGS1)	-4.1	-4.5	-3.8	-4.3
AJ251847	chitinase 3-like 1 (CHI3L1)	-6.1	-7.2	-5.0	-6.1
Extracellular matrix					
AI806793	collagen, type VIII, α2 (COL8A2)	6.9	2.0	5.3	4.2
NM_002380	matrilin 2 (MATN2)	-3.0	-7.1	-2.8	-3.7
NM_002345	lumican (LUM)	-6.7	-6.2	-3.3	-4.8
Growth factor					
X07868	putative insulin-like growth factor II associated protein (IGF2)	9.5	13.1	5.2	7.8
AA583044	bone morphogenetic protein 2 (BMP2)	-3.8	-4.0	-3.3	-3.6
X16323	hepatocyte growth factor (hepapoietin A; scatter factor) (HGF)	-5.6	-3.5	-3.9	-4.2
M13436	inhibin, β A (INHBA)	-4.2	-5.3	-4.2	-4.8
NM_002091	gastrin-releasing peptide (GRP)	-7.2	-7.5	-7.4	-6.8
AF003934	growth differentiation factor 15 (GDF15)	-6.3	-10.5	-6.9	-7.3
NM_000266	Norrie disease (NDP)	-13.0	-4.5	-5.8	-7.7
AI972496	insulin-like growth factor 1 (IGF1)	-12.3	-16.9	-6.4	-13.1
Ion transport					
NM_000219	potassium voltage-gated channel, Isk-related family, member 1 (KCNE1)	8.1	2.3	2.0	4.2
AA551075	potassium channel tetramerization domain containing 12 (KCTD12)	3.0	3.9	2.9	3.3
NM_002246	potassium channel, subfamily K, member 3 (KCNK3)	-2.3	-5.2	-3.3	-3.0
NM_024505	NADPH oxidase, EF-hand calcium binding domain 5 (NOX5)	-2.7	-3.0	-3.4	-3.0
NM_000812	gamma-aminobutyric acid (GABA) A receptor, β1 (GABRB1)	-3.3	-2.6	-3.8	-3.2
AB040120	solute carrier family 39 (zinc transporter), member 8 (SLC39A8)	-7.8	-2.0	-4.4	-4.3
NM_000096	ceruloplasmin (CP)	-4.0	-4.8	-3.7	-4.3

TABLE 3. CONTINUED.

GenBank	Gene title (Symbol)	HTM A fold	HTM B fold	HTM C fold	Mean fold
U73191	potassium inwardly rectifying channel, subfamily J, member 15 (KCNJ15)	-7.9	-7.5	-10.9	-8.8
Kinase					
NM_004438	EPH receptor A4 (EPHA4)	3.9	7.6	12.2	6.4
NM_022740	homeodomain interacting protein kinase 2 (HIPK2)	5.0	4.1	3.8	4.3
NM_030751	SNF1-like kinase (SNF1LK)	5.3	2.7	3.9	3.9
AI992251	ribosomal protein S6 kinase, 90 kDa, polypeptide 2 (RPS6KA2)	4.0	2.4	3.2	3.3
Metallothionein					
R06655	metallothionein 1M (MT1M)	14.1	3.5	10.3	8.9
NM_002450	metallothionein 1X (MT1X)	3.4	4.3	3.3	3.7
Peptidase					
NM_001710	B-factor, properdin (BF)	-3.9	-3.6	-2.4	-3.3
NM_002421	matrix metalloproteinase 1 (MMP1)	-4.9	-2.7	-14.1	-4.4
NM_007038	a disintegrin-like and metalloprotease with thrombospondin type 1 motif, 5 (ADAMTS5)	-2.7	-6.7	-3.4	-4.4
BC006393	carboxypeptidase Z (CPZ)	-2.7	-13.8	-3.7	-4.8
NM_000439	proprotein convertase subtilisin/kexin type 1 (PCSK1)	-16.3	-8.3	-11.9	-11.7
Phosphatase					
AW009884	protein phosphatase 2 (formerly 2A), regulatory subunit A, β isoform (PPP2R1B)	-2.4	-6.5	-5.1	-3.3
Protease inhibitor					
NM_001085	serine (or cysteine) proteinase inhibitor, clade A, member 3 (SERPINA3)	86.0	31.2	52.2	48.2
NM_003064	secretory leukocyte protease inhibitor (SLPI)	24.9	6.3	62.8	34.2
NM_000062	serine (or cysteine) proteinase inhibitor, clade G, member 1 (SERPING1)	4.7	2.1	3.8	3.9
Proteasome					
NM_018324	thioesterase domain containing 1 (THEDC1)	3.1	4.0	2.6	3.2
D42055	neural precursor cell expressed, developmentally down regulated 4 (NEDD4)	1.8	2.1	4.4	3.0
Receptor					
NM_001993	coagulation factor III (F3)	11.3	47.5	26.7	26.2
NM_004633	interleukin 1 receptor, type II (IL1R2)	9.0	58.1	26.9	22.9
NM_014879	purinergic receptor P2Y, G-protein coupled, 14 (P2RY14)	12.4	4.8	6.4	7.5
NM_002029	formyl peptide receptor 1 (FPR1)	6.9	1.1	4.8	3.9
AF064826	glypican 4 (GPC4)	4.7	2.4	4.8	3.7
NM_000361	thrombomodulin (THBD)	3.7	3.7	1.6	3.0
NM_030781	collectin subfamily member 12 (COLEC12)	-2.2	-5.4	-2.3	-3.0
AY029180	plasminogen activator, urokinase receptor (PLAUR)	-6.2	-2.0	-4.0	-3.5
NM_002546	tumor necrosis factor receptor superfamily, member 11b (TNFRSF11B)	-12.6	-7.9	-4.0	-6.6
NM_001338	Coxsackie virus and adenovirus receptor (CXADR)	-4.4	-8.9	-8.0	-7.2
Transcription					
NM_006006	zinc finger and BTB domain containing 16 (ZBTB16)	13.5	14.8	12.3	13.6
AL110191	TSC22 domain family, member 3 (TSC22D3)	6.9	6.2	6.9	6.8
NM_002616	period homolog 1 (PER1)	3.8	3.2	3.2	3.4
NM_015559	SET binding protein 1 (SETBP1)	3.0	2.5	4.8	3.3
NM_004143	Cbp/p300-interacting transactivator, with Glu/Asp-rich carboxy-terminal domain, 1 (CITED1)	-1.1	-5.6	-4.6	-3.3
BF514079	Kruppel-like factor 4 (gut, KLF4)	-2.9	-2.4	-5.0	-3.3
NM_016831	period homolog 3 (PER3)	-2.8	-4.9	-4.4	-3.8
U12767	nuclear receptor subfamily 4, group A, member 3 (NR4A3)	-5.3	-11.5	-1.9	-3.8
AI360875	SRY (sex determining region Y)-box 11 (SOX11)	-2.2	-2.6	-7.2	-3.9
Transport					
M10906	serum amyloid A1 (SAA1)	333.4	37.4	252.9	218.7
NM_030754	serum amyloid A2 (SAA2)	180.2	17.9	145.6	114.0
NM_000275	oculocutaneous albinism II (OCA2)	7.3	2.1	7.6	5.5

Table 3. Continued.

GenBank	Gene title (Symbol)	HTM A fold	HTM B fold	HTM C fold	Mean fold
NM_001647	apolipoprotein D (APOD)	14.8	4.0	10.6	5.3
BF447105	sortilin 1 (SORT1)	3.0	2.0	4.1	3.0
NM_001878	cellular retinoic acid binding protein 2 (CRABP2)	-2.1	-4.3	-2.3	-3.1
NM_003469	secretogranin II (SCG2)	-3.7	-2.9	-4.8	-3.7
Other					
NM_021146	angiopoietin-like 7 (ANGPTL7)	271.9	65.0	116.4	187.0
D88214	myocilin, trabecular meshwork-inducible glucocorticoid response (MYOC)	64.8	7.7	54.8	16.7
NM_014059	response gene to complement 32 (RGC32)	64.6	22.4	8.2	12.3
AL136861	cysteine-rich secretory protein LCCL domain containing 2 (CRISPLD2)	20.9	5.5	7.5	10.6
NM_015385	sorbin and SH3 domain containing 1 (SORBS1)	11.9	2.5	7.7	6.3
AL050264	TU3A protein (TU3A)	4.7	2.5	6.9	4.4
NM_016109	angiopoietin-like 4 (ANGPTL4)	2.3	8.0	2.9	4.1
NM_002923	regulator of G-protein signaling 2, 24 kDa (RGS2)	2.5	2.7	4.4	3.1
AA243659	Family with sequence similarity 49, member A (FAM49A)	2.7	4.1	2.7	3.1
AB020690	paraneoplastic antigen MA2 (PNMA2)	3.0	2.2	3.2	3.1
NM_006444	SMC2 structural maintenance of chromosomes 2-like 1 (yeast) (SMC2L1)	-3.0	-2.7	-3.3	-3.1
BC005961	parathyroid hormone-like hormone (PTHLH)	-1.5	-14.0	-3.5	-3.3
NM_024780	transmembrane channel-like 5 (TMC5)	-3.2	-1.7	-5.7	-3.5
NM_015564	leucine rich repeat transmembrane neuronal 2 (LRRTM2)	-3.3	-2.8	-5.8	-3.6
AF338650	PDZ domain containing 3 (PDZK3)	-6.3	-2.6	-5.4	-4.0
NM_005101	interferon, alpha-inducible protein (clone IFI-15K, G1P2)	-7.0	-2.6	-1.8	-4.0
NM_003810	tumor necrosis factor (ligand) superfamily, member 10 (TNFSF10)	-2.7	-7.1	-3.9	-4.4
AI074333	angiopoietin-like 2 (ANGPTL2)	-3.7	-8.6	-2.8	-4.4
NM_005863	neuroepithelial cell transforming gene 1 (NET1)	-3.0	-7.0	-3.0	-4.4
NM_014890	downregulated in ovarian cancer 1 (DOC1)	-7.3	-5.8	-4.6	-5.9
NM_013409	follistatin (FST)	-13.5	-7.1	-6.9	-8.7
AB024518	chromosome 9 open reading frame 26 (C9orf26)	-3.2	-12.7	-33.7	-17.1

The table lists the GenBank accession number, gene name, fold change within each individual TM cell line and the average of all three cell lines for 111 genes with three fold or greater change in expression determined by microarray analysis. Fold change is relative to untreated cells. Genes are sorted according to functional category.

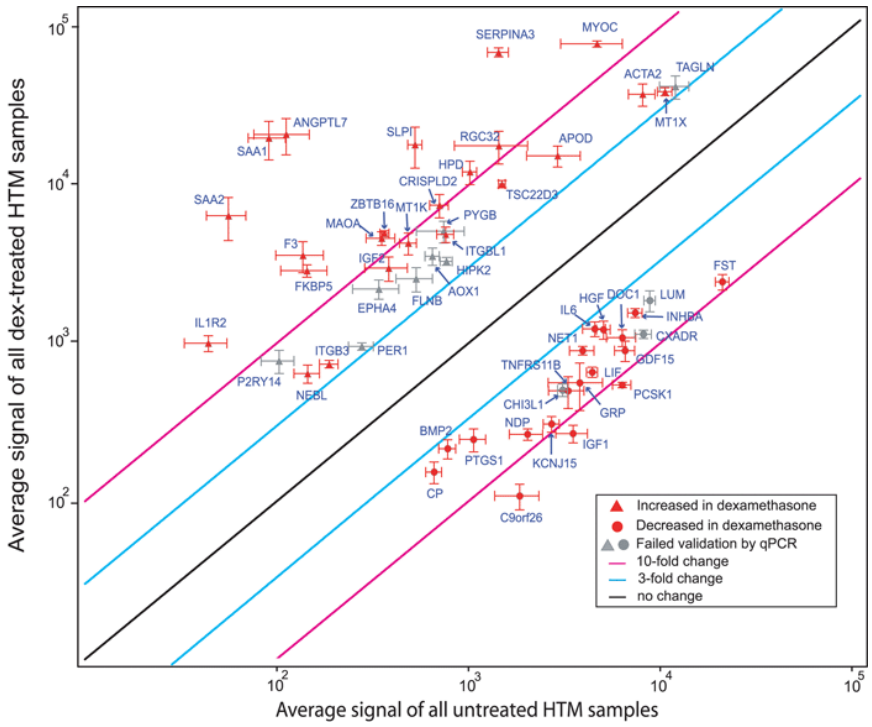

Figure 4. Scatterplot analysis of composite microarray data from three TM cell lines. The logarithmic plot of the composite average GeneChip signal intensities from dexamethasone-treated and untreated cells is shown with error bars representing the standard error of the mean on both axes. Only 52 genes with greater than three fold change in each individual TM cell line are shown. Genes are shown with increased (red triangles) or decreased (red circles) signal intensity in dexamethasone-treated TM cells, relative to untreated cells. Grey symbols indicate genes that failed validation by qPCR (Table 2C). Black, light blue, and pink lines represent fold change boundaries of no change, three fold, and ten fold change, respectively. The Y-axis is the average GeneChip signal intensity from all dexamethasone-treated TM cells; the X-axis is the average GeneChip signal intensity from all untreated TM cells.

old for resolution of signal levels by the GeneChips. MYOC has a particularly wide range in its level of induction, with values reported from 4.3 fold to 148 fold [17-19] which may be due to differences between cell cultures. Using microarray analysis, we observed substantial differences in MYOC expression between cell cultures with fold change values of 64.8-, 7.7-, and 54.8 fold for HTM A, HTM B, and HTM C, respectively. Quantitative PCR results for individual TM cell cultures produced increases in MYOC expression of 1364.6, 27.5, and 186.7 fold for HTM A, HTM B, and HTM C, respectively.

DISCUSSION

Corticosteroid treatment of TM cells has been reported to alter their cellular morphology and function. Ultrastructurally, dexamethasone-treated TM cells demonstrate alterations in CLANs, rearrangements of endoplasmic reticulum, and increased amounts of cell surface extracellular matrix material, including laminin and fibronectin, relative to untreated TM cells [8,28,29]. Increases in integrin receptor expression for laminin, fibronectin, and collagen also occur in response to dexamethasone exposure [29]. To assist us in elucidating the cellular processes and pathways involved in TM function, the

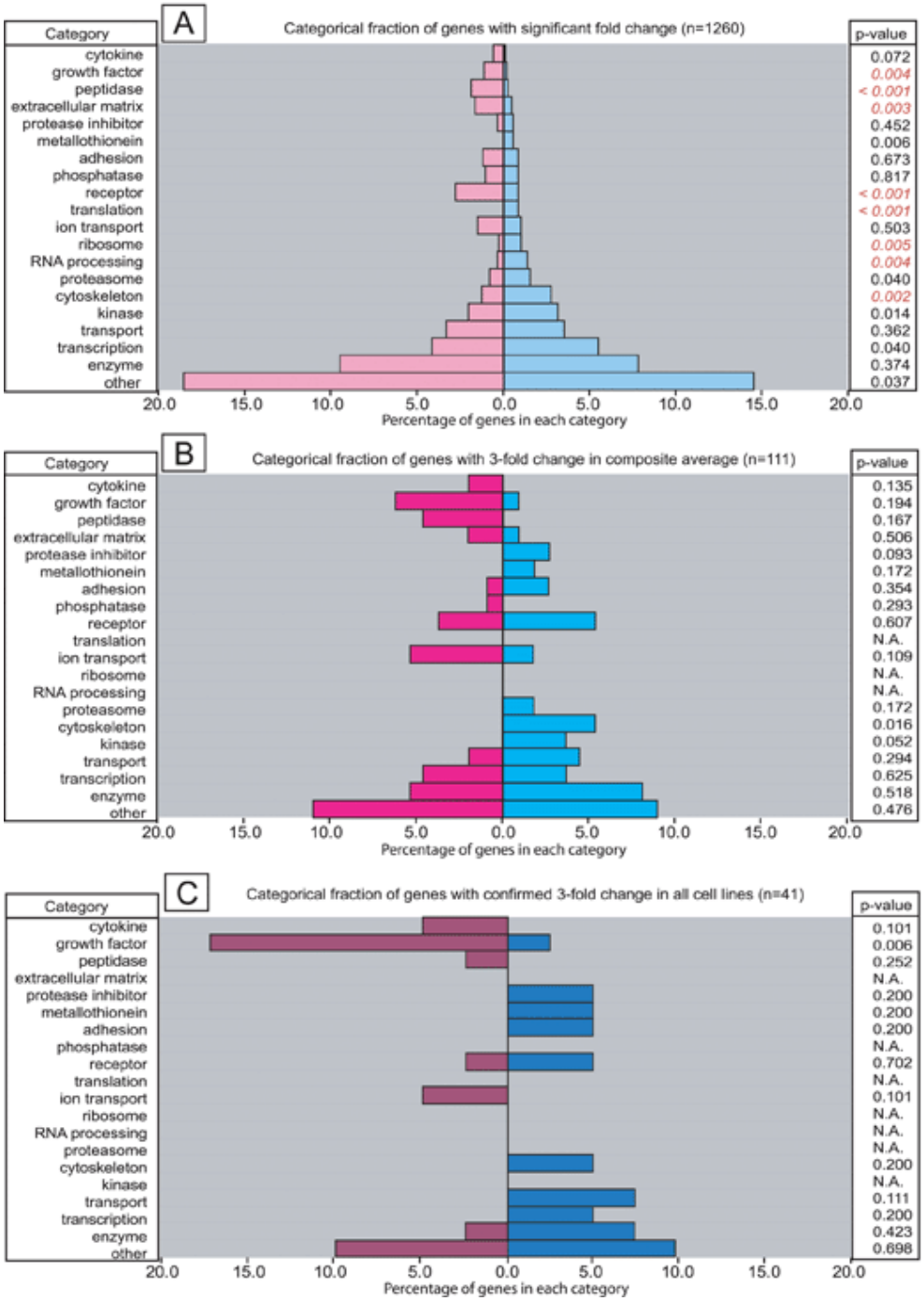

Figure 5. Distribution of genes with increased and decreased signals by functional annotation categories. **A**: 1,260 unique genes with significant increase (n=607) or decrease (n=653) in signal intensity (Figure 3D). **B**: 111 genes from Table 3 that had significant fold change increase (n=58) or decrease (n=53) in the composite data greater than three fold. **C**: 41 genes from Table 2A,B that exceeded a three fold increase (n=23) or decrease (n=18) in signal in all three TM cell cultures. Gene classifications are shown on the left Y-axis; p values on the right Y-axis are from χ^2 test comparing the number of increased and decreased genes in each category to the number of increased and decreased genes in the combined data set. Significant p values are in red italics ($p<0.005$). Genes were classified as described in Methods. Bars to the right of the center line indicate increased signal and bars to the left indicate decreased signal.

genes involved should show changed levels of gene expression when subjected to dexamethasone exposure at levels observable with microarray technology. Additional functional effects resulting from alterations in trafficking, sequestering, turnover rate, or modification of proteins would not be detectable by this technology, so the gene expression changes we observed likely point towards only some of the functional reactions to dexamethasone exposure.

Changes in MYOC expression in response to dexamethasone: MYOC, a gene consistently reported as induced by corticosteroids, produces a protein that may affect more than one of the aforementioned cellular processes. Previous studies have shown that TM cells expressing high levels of myocilin exhibit loss of actin stress fibers and focal adhesions, which is accompanied by reduced TM adhesion to fibronectin, impaired TM motility, and increased TM apoptosis [30,31]. Extracellular myocilin also impairs TM cell attachment to fibronectin [31,32]. These findings raise the possibility that abnormal, myocilin-associated TM-extracellular matrix binding may have effects on other elements including integrins, CLANs, and proteolytic activities. Myocilin impairment of the TM flexibility and plasticity required for maintenance of normal aqueous outflow might contribute to an increase in IOP [31]; however, it remains unclear whether elevated levels of myocilin lead to elevated IOP or not, because organ-culture studies have produced contradictory findings regarding whether increased amounts of nonmutant myocilin protein lead to elevation or decrease of IOP [33,34].

Table 4. Dexamethasone response genes and experimental parameters from other reports

A:

Gene Symbol	Genbank	Lo et al. [17] average fold change (HTM/ONH Astrocytes)	Isibashi et al. [18] mean signal ratio (DEX/Control)	Leung et al. [19] expression ratio (log2)	This study average fold change (all cell lines)
ANGPTL7	NM_021146	28			187.0
SERPINA3	NM_001085	165			48.2
MYOC	D88214	50	24	4.32 (qPCR)	16.7
MAOA	AA923354		2.4		13.1
ACTG2	NM_001615	30			9.4
APOD	NM_001647	22			5.3
MT1X	NM_002450			1.9	3.7
TAGLN	NM_003186			1.53	3.5
DHCR24	NM_014762		2.1		2.5
KCNB1	L02840		0.5		2.4
BNIP3	NM_004052		2.2		2.3
LTBP2	NM_000428		3.1		2.2
IGFBP2	NM_000597	57	4.9	1.7	2.1
TPM2	NM_003289		2.1		2.1
AKR1C3	AB018580	43			1.5
ATF4	NM_001675			0.55	1.5
MORF4L2	NM_012286		2		1.5
ACTR3	NM_005721		0.5		1.4
CST3	NM_000099			1.95	1.4
SCD	AB032261		2.1		1.4
AKR1B10	NM_020299		3.5		1.3
LDHA	NM_005566			1.61	1.2
HSPA5	AF216292			0.58	-1.3
IGFBP4	NM_001552		2.5		-1.3
HADHB	NM_000183		0.5		-1.4
PER2	NM_022817		2		-1.4
DCN	NM_001920		3.5		-1.5
FBLN1	NM_006486		2.8		-1.8
FLRT2	NM_013231		0.4		-2.5
CRABP2	NM_001878		0.3		-3.1
SCG2	NM_003469		0.4	0.64	-3.7
CHI3L1	AJ251847	33			-6.1

B:

Study	TM cell lines	Age of donors	Cell passage	Dex exposure	Number of genes screened	Array type
Lo et al. [17]	2	not reported	4-6	10 days	9,330 unique clusters	Oligonucleotide (U95Av2)
Ishibashi et al. [18]	4	7 to 28 years	4-5	7 days	2,400	cDNA (NEN)
Leung et al. [19]	1	not reported	8	10 days	2,400	cDNA (NEN)
This work	3	12, 16, 17 years	5	21 days	13,507 unique clusters	Oligonucleotide (U133A)

A: Genes with differential expression following dexamethasone treatment identified by other groups are listed with gene symbol, GenBank accession number and the measurement of differential expression used in that study. The average fold calculation is based on dexamethasone-treated HTM compared to dexamethasone-treated optic nerve head astrocytes in Lo et al. [17]. **B**: Experimental parameters for the three recent microarray studies described in Table 4A.

Genes with potential involvement in CLAN formation in response to dexamethasone: Others have shown altered formation of TM CLANs from dexamethasone treatment [8,28] The recognition of specific actin-associated TM genes that are selectively affected by corticosteroid treatment indicates that the genes may play a role in mechanisms that modify TM CLANs, leading to abnormal TM function and reduced aqueous outflow. In addition to a 9.4 fold change in signal from actin gene ACTG2, we found corticosteroids induced alterations in the expression of genes encoding several other TM proteins that either form part of or interact with the actin cytoskeleton. Actin genes ACTA2 and ACTC, filamins A, B, and C (FLNA, FLNB, FLNC), transgelin (TAGLN) [35], nonmuscle heavy myosin peptide (MYH9), caldesmon 1 (CALD1), and tropomyosin 2β (TPM2) were among those showing significant increases (Appendix 1). FLNA and FLNB seem plausible candidates for the CLAN alterations seen following corticosteroid treatment of TM cells because filamins connect actin fibers in crossed rather than parallel formations [36]. Corticosteroid induction of filamins may be expected to reorganize TM CLANs and their plasmalemma attachments, inhibiting TM cell retraction due to greater strength of cell-to-cell and cell-to-substrate binding [37]. Filamins also subserve other functions that may affect TM-extracellular matrix binding and cellular migration [38]. The intracellular domain of filamins binds to transmembrane beta-1 integrins, permitting extracellular signals to modify CLANs, focal adhesions, and fiber stress formation [39] and to activated RalA protein, a small GTPase, which promotes the extension of cellular filopodia [38]. Thus, corticosteroid-induced alterations in filamin expression might interfere with normal cellular signaling required for coordinated cellular retraction and junctional separation, which is important to normal TM cell functioning [37]. Increases in nonmuscle myosin may also affect TM-extracellular matrix interactions by mediating TGF-β1-induced collagen contraction, which is associated with actin stress fiber formation and enhanced TM motility [40]. In animal eyes, disruption of myosin binding by inhibiting myosin light chain kinase reduces intraocular pressure, presumably by altering TM shape and causing TM retraction from the extracellular matrix by disrupting focal adhesions and intracellular actin bundling [41].

Predicted changes in proteolysis in TM cells in response to dexamethasone: TM treatment with corticosteroids leads to reductions in extracellular proteolytic activity of stromelysin, type IV collagenase, and tissue plasminogen activator (Appendix 1) [42]. Our data support a model of reduced nonproteasomal proteolysis in TM cells exposed to dexamethasone based on the large changes in signal levels for some genes that affect levels of proteolysis. We see increases among protease inhibitor genes that show altered signal levels. One, SLPI (serine leukocyte protease inhibitor), showed an increase of 34 fold. Another, SERPINA3, also known as AACT (α-1-antichymotrypsin), was among the most highly induced genes observed, with an average induction of over a hundred fold (Table 2A). Differences in the technologies used make it impossible to make quantitative comparisons with the results of Nguyen et al. [12] who reported a "minor" induction of SERPINA3 when they exposed TM cells to dexamethasone.

An increase in protease inhibitors is complemented by decreases in signal levels for a number of genes that encode proteases. We found that both MMP1 (collagenase) and CHI3L1, whose product is involved in tissue remodeling, were reduced by TM exposure to corticosteroids. A decrease in PCSK1 (Table 2A), which has been previously shown to cleave some hormone precursors, points toward a possible reduction in some specific cleavage events. The conclusion that overall proteolysis decreases is strengthened by the observation of decreased transcript levels for several disintegrin and disintegrin-like proteins in the ADAM family of proteins (Appendix 1). In contrast, we see modest increases in a number of genes involved in the specific proteolytic pathway for proteasomal degradation of ubiquitin-tagged proteins (Appendix 1).

Changes in genes encoding extracellular matrix proteins: Overall, the decreased expression of transcripts encoding proteases, in conjunction with the increased levels of transcripts encoding protease inhibitors, leads us to suggest that a general reduction of proteolysis may occur in TM cells in response to dexamethasone. We expect a decrease in proteolysis to affect the turnover and accumulation of other proteins, and that altered proteolysis might affect levels of proteins for some genes that do not show altered transcript levels in our assay system. Thus, observed increased levels of transcripts encoding extracellular matrix proteins, such as collagen type VIII (COL8A2), fibronectin (FN1), angiopoietin-like factor (ANGPTL7), and glypican 3 (GPC3, Appendix 1), may be enhanced at the protein level by reduced proteolysis leading to increased deposition of materials in the extracellular matrix. If proteolysis is decreased then the changes in transcript level may only partly reflect the real changes in amount of protein product present in the cell. Additional experiments are needed to evaluate how altered levels of proteolysis may contribute to the observed changes in the extracellular matrix of the TM in response to dexamethasone [43,44], and to identify the key functions and structures within the TM cell that are affected. Overall reduction in proteolysis might be expected to result in deficient TM remodeling of the extracellular matrix that may prevent removal of damaged components leading to TM cell dysfunction.

IGFBP2 is one of several growth factors that we found to have decreased signal following dexamethasone treatment (Table 3, Table 2). Growth factor genes with decreased signals accounted for 1.1% of the total significant changes, while only 0.2% of the total significant changes were accounted by increased signals from growth factor transcripts (Figure 5A, Appendix 1). When we consider genes with a minimum three fold change (Figure 5B), more growth factors were decreased (6.3%) in comparison to those with increased expression (0.9%, p=0.021). Under the most stringent data filter (Figure 5C) that required a minimum three fold change in every cell culture, decreased signals from growth factor genes accounted for 17.1% of the total change while 2.4% represented growth factors with increased signal (p=0.006). In keeping with this ob-

servation, insulin-like growth factor 1 (IGF1) expression was decreased by 13.1 fold; in contrast expression of insulin-like growth factor 2 (IGF2) increased by 7.8 fold. Both genes produced larger variation from qPCR (Table 2A,B). These results may indicate involvement of multiple growth factors in TM responses to dexamethasone.

Changes in acute phase reaction proteins: We identified increases in the expression of several genes whose role in TM function remain unknown. Two genes showing the largest change in response to dexamethasone are the serum amyloid genes, SAA1 and SAA2, with signal differences in excess of a hundred fold (Table 2A). The increase in SAA1 and SAA2, but not SAA4, could indicate a coordinated regulation of these head to head, especially since SAA1 and SAA2 are close together in a head to head arrangement with regulatory regions between them [45]. SAA1 and SAA2 are members of an acute phase response family of proteins whose systemic concentrations dramatically change during the initial inflammatory process [46,47]. Additional acute phase reaction proteins for which we observed significant changes include fibronectin, plasminogen activator urokinase receptor (PLAUR), IGF1, ceruloplasmin (CP), interleukin 6 (IL6), and a number of the serine protease inhibitors and metallothioneins (Appendix 1). Thus, among the TM responses to dexamethasone we find changes in a number of proteins often considered to be markers for inflammatory processes, but the significance of changes in these proteins remains unclear in the context of this system.

Genes identified by four different studies of TM responses to dexamethasone: Three recent studies used microarray technology to quantitate gene expression in dexamethasone-treated TM cells [17-19]. Table 4A presents probes identified by prior studies that are also present on our list of 1,260 significantly increased genes (Appendix 1). Our study findings best match the results of Lo et al. [17], which used U95Av2 Affymetrix GeneChips and identified 15 TM specific genes with greater than 20 fold increase in expression following dexamethasone treatment when comparing dexamethasone-treated TM cells to dexamethasone-treated optic nerve head astrocytes (Table 4B). In contrast, we identified only seven genes with signal increases greater than 20 fold across all cell cultures (Table 2A, Table 4A). Seven genes reported by Lo et al. [17] (ACTG2, AKR1C3, APOD, ANGPTL7, IGFBP2, MYOC, and SERPINA3) also showed significant signal increases in our analysis. Conversely, CHI3L1, which showed a 33 fold increase in Lo et al. [17], was significantly reduced in our U133A GeneChip and qPCR results (Table 2C). The remaining genes reported in their study were statistically unchanged in ours (data not shown). We found a few genes (Table 2) that consistently showed greater than three fold changes including MAOA, RGC32, and SAA1 that do not appear on the list of Lo et al. [17] even though the genes are present on the U95Av2 GeneChips that they used. Either, the genes had expression levels below their cutoff point of 20 fold or the expression of these genes may be equally elevated in both dexamethasone-treated TM and optic nerve head astrocytes thus masking the difference relative to our study. Experimental factors such as the substantially shorter exposure to dexamethasone are known to have a major impact on the expression of myocilin. Variables that are difficult to standardize between studies, such as the genetic background of donors, tissue collection methods, or propagation of the cell cultures, are other sources of variation.

Ishibashi et al. [18] used MicroMax cDNA microarrays (Perkin Elmer Life Sciences, Boston, MA) containing 2,400 genes. They identified 30 up regulated and 34 down regulated genes at a two fold or greater threshold in dexamethasone-treated TM cells. We cross-indexed 61 of these MicroMax cDNAs to the corresponding Affymetrix probes and found that only MYOC and MAOA are present on our list of 41 genes with significant signal changes greater than three fold across all three TM cell cultures (Table 2A, Table 4A). An additional 12 genes identified by Ishibashi et al. [18] were also considered to have significant differences in signal under less stringent criterion than ours (Table 4A). Several genes reported by Ishibashi [18] had changes in expression that conflict with our findings. They report decreased expression for ACTR3 and KCNB1 and increased expression for IGFBP4, FBLN1, DCN, and PER2, which were significantly expressed in the opposite direction but below a three fold threshold in our study (Table 4A). The remaining genes identified in their study were considered absent under both untreated and dexamethasone-treated conditions (11 genes) or were found to be statistically unchanged (30 genes) by us (data not shown).

The same 2,400-gene microarray technology was used by Leung et al. [19] to examine dexamethasone response in a single TM cell culture at the eighth passage (Table 4). Their study identified 14 differentially expressed genes of which MYOC, MT1X, and TAGLN were also present on our list (Table 2A,C). Additional genes identified by Leung et al. [19] produced increased (CST3, LDHA, and IGFBP2) or decreased (HSPA5 and SCG2) signals following dexamethasone treatment also can be found in our list of 1,260 genes with statistically significant signal change (Table 4A). The decreased expression of ATF4 reported by Leung et al. [19] was contrary to our findings, which indicated a modest, yet significantly increased signal (Figure 3D). They report five other genes that appear unchanged or failed to generate a signal in our GeneChip arrays (data not shown). The substantial differences between our findings and those of Ishibashi et al. [18] and Leung et al. [19] might be attributable to the smaller number of genes they screened using a different microarray signal normalization and key experimental differences described above.

Although we identified significant changes in the expression of many TM genes following a course of dexamethasone treatment, we find that only two genes, MYOC and insulin-like growth factor binding protein 2 (IGFBP2), were identified by all four studies that have evaluated gene expression changes in response to dexamethasone. Our study, and that of Lo et al. [17], found seven genes with elevated expression (Table 4A). Six of these genes have an impact on cellular proliferation and survival (AKR1C3 and APOD) or on structural elements such as actin (ACTG2) extracellular matrix (ANGPTL7), or matrix remodeling (IGFBP2 and SERPINA3).

In summary, the response of TM to dexamethasone treatment causes relatively large expression change in genes forming part of or interacting with the actin cytoskeleton. Additionally, changes in genes influencing proteolysis suggest the involvement of corticosteroids in altering the regulation of the stability and turnover of gene products in addition to regulation of transcription.

ACKNOWLEDGEMENTS

This work was supported by NIH EY07003 (Core grant), NIH EY09580 (JER), NIH T32 HG00040 (CMK), Career Development Award from RPB (SEM), NIH EY11405 (DV), NIH EY09441 (VME), and an unrestricted grant from Research to Prevent Blindness, Inc. The authors have no financial or proprietary conflicts relevant to the content of this paper.

REFERENCES

1. Armaly MF. Effect of corticosteroids on intraocular pressure and fluid dynamics. I. The effect of dexamethasone in the normal eye. Arch Ophthalmol 1963; 70:482-91.
2. Francois J. Corticosteroid glaucoma. Ann Ophthalmol 1977; 9:1075-80.
3. Aggarwal RK, Potamitis T, Chong NH, Guarro M, Shah P, Kheterpal S. Extensive visual loss with topical facial steroids. Eye 1993; 7:664-6.
4. Baratz KH, Hattenhauer MG. Indiscriminate use of corticosteroid-containing eyedrops. Mayo Clin Proc 1999; 74:362-6.
5. Dreyer EB. Inhaled steroid use and glaucoma. N Engl J Med 1993; 329:1822.
6. Weinreb RN, Polansky JR, Kramer SG, Baxter JD. Acute effects of dexamethasone on intraocular pressure in glaucoma. Invest Ophthalmol Vis Sci 1985; 26:170-5.
7. Weinreb RN, Bloom E, Baxter JD, Alvarado J, Lan N, O'Donnell J, Polansky JR. Detection of glucocorticoid receptors in cultured human trabecular cells. Invest Ophthalmol Vis Sci 1981; 21:403-7.
8. Clark AF, Wilson K, McCartney MD, Miggans ST, Kunkle M, Howe W. Glucocorticoid-induced formation of cross-linked actin networks in cultured human trabecular meshwork cells. Invest Ophthalmol Vis Sci 1994; 35:281-94.
9. Iqbal Z, Muhammad Z, Shah MT, Bashir S, Khan T, Khan MD. Relationship between the concentration of copper and iron in the aqueous humour and intraocular pressure in rabbits treated with topical steroids. Clin Experiment Ophthalmol 2002; 30:28-35.
10. Zhou L, Li Y, Yue BY. Glucocorticoid effects on extracellular matrix proteins and integrins in bovine trabecular meshwork cells in relation to glaucoma. Int J Mol Med 1998; 1:339-46.
11. el-Shabrawi Y, Eckhardt M, Berghold A, Faulborn J, Auboeck L, Mangge H, Ardjomand N. Synthesis pattern of matrix metalloproteinases (MMPs) and inhibitors (TIMPs) in human explant organ cultures after treatment with latanoprost and dexamethasone. Eye 2000; 14:375-83.
12. Nguyen TD, Chen P, Huang WD, Chen H, Johnson D, Polansky JR. Gene structure and properties of TIGR, an olfactomedin-related glycoprotein cloned from glucocorticoid-induced trabecular meshwork cells. J Biol Chem 1998; 273:6341-50.
13. Polansky JR, Fauss DJ, Chen P, Chen H, Lutjen-Drecoll E, Johnson D, Kurtz RM, Ma ZD, Bloom E, Nguyen TD. Cellular pharmacology and molecular biology of the trabecular meshwork inducible glucocorticoid response gene product. Ophthalmologica 1997; 211:126-39.
14. Shimizu S, Lichter PR, Johnson AT, Zhou Z, Higashi M, Gottfredsdottir M, Othman M, Moroi SE, Rozsa FW, Schertzer RM, Clarke MS, Schwartz AL, Downs CA, Vollrath D, Richards JE. Age-dependent prevalence of mutations at the GLC1A locus in primary open-angle glaucoma. Am J Ophthalmol 2000; 130:165-77.
15. Lutjen-Drecoll E, May CA, Polansky JR, Johnson DH, Bloemendal H, Nguyen TD. Localization of the stress proteins alpha B-crystallin and trabecular meshwork inducible glucocorticoid response protein in normal and glaucomatous trabecular meshwork. Invest Ophthalmol Vis Sci 1998; 39:517-25.
16. Fingert JH, Heon E, Liebmann JM, Yamamoto T, Craig JE, Rait J, Kawase K, Hoh ST, Buys YM, Dickinson J, Hockey RR, Williams-Lyn D, Trope G, Kitazawa Y, Ritch R, Mackey DA, Alward WL, Sheffield VC, Stone EM. Analysis of myocilin mutations in 1703 glaucoma patients from five different populations. Hum Mol Genet 1999; 8:899-905.
17. Lo WR, Rowlette LL, Caballero M, Yang P, Hernandez MR, Borras T. Tissue differential microarray analysis of dexamethasone induction reveals potential mechanisms of steroid glaucoma. Invest Ophthalmol Vis Sci 2003; 44:473-85.
18. Ishibashi T, Takagi Y, Mori K, Naruse S, Nishino H, Yue BY, Kinoshita S. cDNA microarray analysis of gene expression changes induced by dexamethasone in cultured human trabecular meshwork cells. Invest Ophthalmol Vis Sci 2002; 43:3691-7.
19. Leung YF, Tam PO, Lee WS, Lam DS, Yam HF, Fan BJ, Tham CC, Chua JK, Pang CP. The dual role of dexamethasone on anti-inflammation and outflow resistance demonstrated in cultured human trabecular meshwork cells. Mol Vis 2003; 9:425-39.
20. Alvarado JA, Wood I, Polansky JR. Human trabecular cells. II. Growth pattern and ultrastructural characteristics. Invest Ophthalmol Vis Sci 1982; 23:464-78.
21. Polansky JR, Weinreb RN, Baxter JD, Alvarado J. Human trabecular cells. I. Establishment in tissue culture and growth characteristics. Invest Ophthalmol Vis Sci 1979; 18:1043-9.
22. Rozsa FW, Shimizu S, Lichter PR, Johnson AT, Othman MI, Scott K, Downs CA, Nguyen TD, Polansky J, Richards JE. GLC1A mutations point to regions of potential functional importance on the TIGR/MYOC protein. Mol Vis 1998; 4:20.
23. Liu G, Loraine AE, Shigeta R, Cline M, Cheng J, Valmeekam V, Sun S, Kulp D, Siani-Rose MA. NetAffx: Affymetrix probesets and annotations. Nucleic Acids Res 2003; 31:82-6.
24. Bussey KJ, Kane D, Sunshine M, Narasimhan S, Nishizuka S, Reinhold WC, Zeeberg B, Ajay W, Weinstein JN. MatchMiner: a tool for batch navigation among gene and gene product identifiers. Genome Biol 2003; 4:R27.
25. Dennis G Jr, Sherman BT, Hosack DA, Yang J, Gao W, Lane HC, Lempicki RA. DAVID: Database for Annotation, Visualization, and Integrated Discovery. Genome Biol 2003; 4:P3.
26. Irizarry RA, Hobbs B, Collin F, Beazer-Barclay YD, Antonellis KJ, Scherf U, Speed TP. Exploration, normalization, and summaries of high density oligonucleotide array probe level data. Biostatistics 2003; 4:249-64.
27. Bolstad BM, Irizarry RA, Astrand M, Speed TP. A comparison of normalization methods for high density oligonucleotide array data based on variance and bias. Bioinformatics 2003; 19:185-93.
28. Wilson K, McCartney MD, Miggans ST, Clark AF. Dexamethasone induced ultrastructural changes in cultured human trabecular meshwork cells. Curr Eye Res 1993; 12:783-93.

29. Dickerson JE Jr, Steely HT Jr, English-Wright SL, Clark AF. The effect of dexamethasone on integrin and laminin expression in cultured human trabecular meshwork cells. Exp Eye Res 1998; 66:731-8.
30. Wentz-Hunter K, Shen X, Okazaki K, Tanihara H, Yue BY. Overexpression of myocilin in cultured human trabecular meshwork cells. Exp Cell Res 2004; 297:39-48.
31. Wentz-Hunter K, Kubota R, Shen X, Yue BY. Extracellular myocilin affects activity of human trabecular meshwork cells. J Cell Physiol 2004; 200:45-52.
32. Filla MS, Liu X, Nguyen TD, Polansky JR, Brandt CR, Kaufman PL, Peters DM. In vitro localization of TIGR/MYOC in trabecular meshwork extracellular matrix and binding to fibronectin. Invest Ophthalmol Vis Sci 2002; 43:151-61.
33. Caballero M, Gonzalez P, Russell P, Rowlette LLS, Borras T. Adenoviral gene transfer of a single domain of the TIGR/MYOC protein to the human perfused anterior segment cultures. Invest Ophthalmol Vis Sci 1999; 40:S597.
34. Fautsch MP, Bahler CK, Vrabel AM, Howell KG, Loewen N, Poeschla EM, Johnson DH. Recombinant myocilin purified from human trabecular meshwork cells increases outflow resistance in human anterior segments but only in the presence of aqueous humor. ARVO Annual Meeting; 2005 May 1-5; Fort Lauderdale (FL).
35. Shapland C, Hsuan JJ, Totty NF, Lawson D. Purification and properties of transgelin: a transformation and shape change sensitive actin-gelling protein. J Cell Biol 1993; 121:1065-73.
36. Pudas R, Kiema TR, Butler PJ, Stewart M, Ylanne J. Structural basis for vertebrate filamin dimerization. Structure 2005; 13:111-9.
37. O'Brien ET, Perkins SL, Roberts BC, Epstein DL. Dexamethasone inhibits trabecular cell retraction. Exp Eye Res 1996; 62:675-88.
38. Couillard-Despres S, Winkler J, Uyanik G, Aigner L. Molecular mechanisms of neuronal migration disorders, quo vadis? Curr Mol Med 2001; 1:677-88.
39. Peterson JA, Sheibani N, David G, Garcia-Pardo A, Peters DM. Heparin II domain of fibronectin uses alpha4beta1 integrin to control focal adhesion and stress fiber formation, independent of syndecan-4. J Biol Chem 2005; 280:6915-22.
40. Nakamura Y, Hirano S, Suzuki K, Seki K, Sagara T, Nishida T. Signaling mechanism of TGF-beta1-induced collagen contraction mediated by bovine trabecular meshwork cells. Invest Ophthalmol Vis Sci 2002; 43:3465-72.
41. Honjo M, Inatani M, Kido N, Sawamura T, Yue BY, Honda Y, Tanihara H. A myosin light chain kinase inhibitor, ML-9, lowers the intraocular pressure in rabbit eyes. Exp Eye Res 2002; 75:135-42.
42. Snyder RW, Stamer WD, Kramer TR, Seftor RE. Corticosteroid treatment and trabecular meshwork proteases in cell and organ culture supernatants. Exp Eye Res 1993; 57:461-8.
43. Clark AF, Wilson K, de Kater AW, Allingham RR, McCartney MD. Dexamethasone-induced ocular hypertension in perfusion-cultured humaneyes. Invest Ophthalmol Vis Sci 1995; 36:478-89.
44. Johnson D, Gottanka J, Flugel C, Hoffmann F, Futa R, Lutjen-Drecoll E. Ultrastructural changes in the trabecular meshwork of human eyes treated with corticosteroids. Arch Ophthalmol 1997; 115:375-83.
45. Sellar GC, Oghene K, Boyle S, Bickmore WA, Whitehead AS. Organization of the region encompassing the human serum amyloid A (SAA) gene family on chromosome 11p15.1. Genomics 1994; 23:492-5.
46. Tillett WS, Francis T Jr. Serological reactions in pneumonia with a non-protein somatic fraction of Pneumonococcus. J Exp Med 1930; 52:561-72.
47. Gabay C, Kushner I. Acute-phase proteins and other systemic responses to inflammation. N Engl J Med 1999; 340:448-54. Erratum in: N Engl J Med 1999; 340:1376.

The appendix is available in the online version of this article at http://www.molvis.org/molvis/v12/a14/.

The print version of this article was created on 27 Feb 2006. This reflects all typographical corrections and errata to the article through that date. Details of any changes may be found in the online version of the article.